# High performance organic polymer light-emitting heterostructure devices

Y. He,[a] S. Gong, R. Hattori, and J. Kanicki
*Electronics Manufacturing Laboratory, Center for Integrated Microsystems, University of Michigan, Ann Arbor, Michigan 48109*

(Received 19 October 1998; accepted for publication 24 February 1999)

We report a high performance electroluminescence device based on bi-layer conjugated polymer structures consisting of a hole transporting (amine-fluorene) and an emissive (benzothiadiazole-fluorene) polymer layers prepared by the spin-coating technique on the glass substrate. Devices showed green emission with an electroluminescence peak located at around 545 nm and a full width at half maximum of about 80 nm. Our devices have also shown a high brightness ($\sim$10 000 cd/m$^2$ at 0.84 mA/mm$^2$), good emission efficiency ($\sim$14.5 cd/A) and luminous efficiency (2.26 lm/W), a large external quantum efficiency (3.8%), and a reasonable forward-to-reverse bias current rectification ratio ($>10^3$ at $\pm$25 V). © *1999 American Institute of Physics.* [S0003-6951(99)04316-8]

The first demonstration of the electroluminescence from the conjugated polymer thin films in 1990 (Ref. 1) has ignited a worldwide attention of the polymeric light-emitting diodes (OLEDs). The inherent thin-film structure of the OLED makes it a particularly attractive candidate for the flat panel display (FPD) applications,[2] which is now dominated by liquid crystal displays (LCDs). Since 1990, the performance of the single layer polymer based OLEDs has been improved dramatically. Both red and green emission devices with the external quantum efficiency higher than $\sim$1% and luminous efficiency greater than $\sim$2 lm/W have been reported,[3,4] while the blue emission devices with external quantum efficiency as high as 3% have also been presented.[5] All these devices use reactive, air-unstable, low work function materials as the cathode electrodes to achieve a high electron injection level. Efforts such as using another stable protection cover layer on the top of the cathode electrode or encapsulating the device in the inert gas atmosphere are employed to minimize the oxidation pace of the low work function materials and to improve the device stability. However, the low work function electrode may still act as a fast diffusing species, which could potentially affect the device stability.[6] On the other hand, devices using air-stable metals, e.g., Al, suffer from a high operating voltage and low efficiencies, although the use of a stable metal is potentially beneficial to the development of the process integration and packaging steps needed for the display applications.

In 1993, Greenham *et al.* reported an efficient OLED heterostructure configuration in which a double layer was formed to achieve a better charge injection and charge confinement.[7] For this heterostructure configuration, the OLED internal quantum efficiency has been improved from 0.2% up to 4% using calcium as the cathode material. The electrical driving field has also been reduced from $\sim$1.2 to $\sim 0.4\times 10^6$ V/cm to obtain a current density of 5 mA/cm$^2$.[7] However, in general the OLEDs efficiencies are still not high enough to challenge the LCD dominated FPD market.[8] It is estimated that an external quantum efficiency exceeding 7.5% and an aperture ratio (the fraction of the light-emitting area in a pixel) above 65% is required for OLED displays to compete with the thin-film transistor (TFT) driven LCDs.[8]

In this letter, we report a high performance heterostructure OLED using air-stable aluminum as the cathode electrode. The obtained device efficiencies are much higher than the values reported for the other polymer OLEDs.[3–5,9]

The transparent anode, i.e., indium tin oxide (ITO), was sputtered on the glass substrates, which were cleaned in the sequential ultrasonic baths of nanostrip (a mixture of sulfuric acid, peroxymonosulfuric acid, and hydrogen peroxide), deionized (DI) water, and isopropanol. The electrode definition of ITO was done either via a shadow mask during the sputtering or via photolithographic steps after the sputtering. The thermally annealed ITO thin film ($\sim$1600 Å) usually had a sheet resistance lower than 30 $\Omega/\square$. Its typical transparency was higher than 85% throughout the visible range (400–800 nm). After postsputter thermal annealing, the ITO covered glass substrates were cleaned again by the isopropanol ultrasonic bath and then irradiated by ultraviolet (UV)–ozone before the deposition of polymer layers. Two polymers, a hole transport (amine-fluorene) polymer and an emissive (benzothiadiazole-fluorene) polymer, were used in this study. To form a bilayer OLED structure, polymer A (hole transporting polymer, $\sim$70 Å thick) and polymer B (emissive polymer, $\sim$1400 Å thick) were spin coated sequentially on the patterned anode substrate. The sample was then transferred to a vacuum chamber ($\sim 10^{-6}$ Torr) for the top cathode electrode (Al) evaporation to form the sandwiched structure. The Al cathode was deposited on the substrate through a shadow mask.

The electroluminescence (EL) of OLEDs was measured by a charge-coupled device (CCD) spectral analyzer through optical fibers. The CCD spectral analyzer has been calibrated by a Labsphere USS-600 Uniform Source System incorporated with a calibration lamp and a motorized variable attenuator. During the EL measurement, the OLED and the optical fiber were placed at different sides of a convex lens. Both the distance between the lens and the OLED and the

[a]Author to whom correspondence should be addressed. Electronic mail: heyi@engin.umich.edu

 

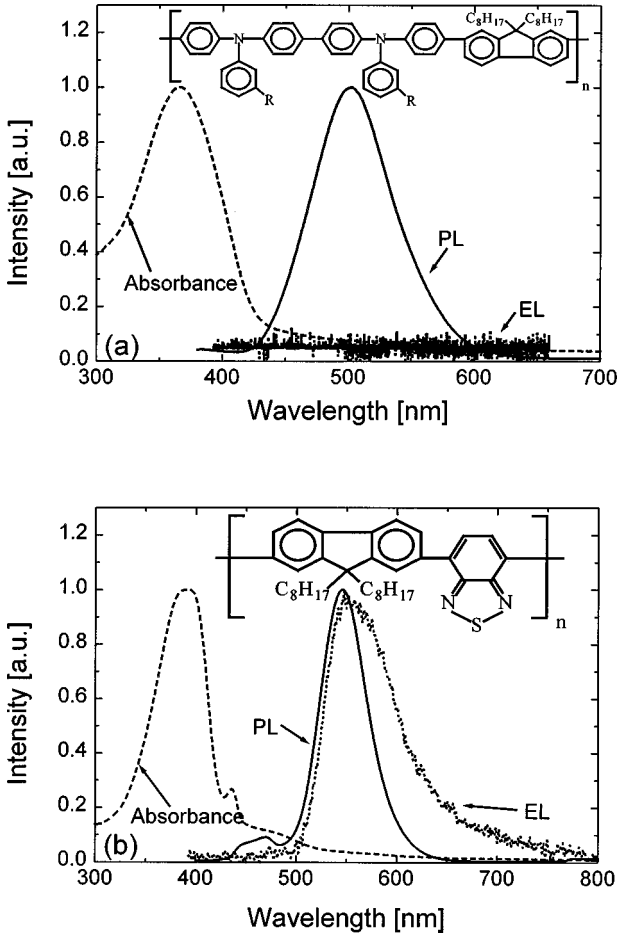


FIG. 1. Absorbance, photoluminescence, and electroluminescence spectra of (a) amine-fluorene (hole transport polymer) thin film; (b) benzothiadiazole-fluorene (emissive polymer) thin film. The chemical structures of both polymers are shown (inset).

distance between the lens and the optical fiber are two times the focal length of the lens. The actual luminance (candelas per square meter) and radiant power of the OLEDs were corrected by assuming the angular distribution of the Lambertian emission.[10] No corrections were made for the absorption of the lens and glass substrate, refraction/reflection at the polymer–glass–air interfaces, or other effects that could decrease the light emission intensity from the OLEDs. The current–voltage characteristics of the OLEDs were measured in a vacuumed metal box with shielded cables connecting the voltage source, current meter, and the probes inside the measurement box. The absorption and the photoluminescence (PL) spectra were collected by a CARY UV-visible spectrophotometer and a Shimadzu 4121, respectively. Films about 100 nm and $1-2$ $\mu$m thick have been used for absorption and PL measurements, respectively.

Figures 1(a) and 1(b) illustrate the absorbance, PL, and EL spectra of the polymer A (amine-fluorene) and B (benzothiadiazole-fluorene), respectively. The inset figures show the chemical structures of these two polymers. The EL spectra were obtained from the Al/polymer/ITO/glass structure. The EL emission of the polymer B ($\sim$1400 Å) clearly shows a peak located at around 545 nm, which is consistent with its PL counterpart. No electroluminescence has been observed from the Al/polymer A ($\sim$200 Å)/ITO/glass structure at a current density up to 7.0 mA/mm$^2$. The absence of

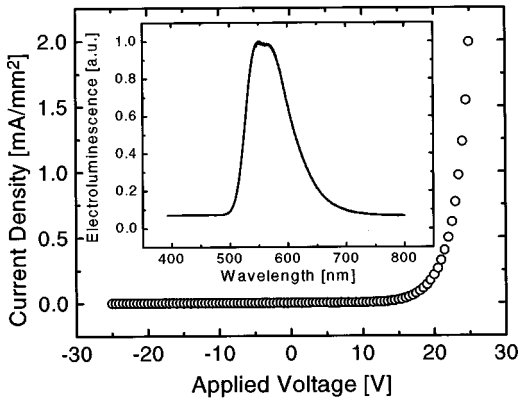


FIG. 2. *I–V* characteristics and the electroluminescence spectra (the inset) of the bilayer OLEDs. The device structure is Al (2000 Å)/Polymer B (1400 Å)/Polymer A (70 Å)/ITO (1600 Å).

EL in the hole transporting polymer is probably due to the low electron mobility and the existence of an excessive hole concentration in such a material. As a result, the lifetime of the injected electrons (minority carriers) from Al electrode is greatly reduced. Therefore, similar to what happens in a *p*-type crystalline semiconductor, the majority of the injected holes from ITO contact will reach the Al electrode through band conduction without encountering a large density of electrons needed for the electron–hole recombination. In addition, most of the singlet excitons will be localized very close to the Al cathode electrode, where the nonradiative decay processes will more likely occur. The existence of the defect centers and other quenching sites near the Al/polymer interface will further enhance the nonradiative decay processes. As a result, only a very small portion of the injected electrons/holes can successfully contribute to electroluminescence (electron–hole recombination rate is very low) and a very high current density might be needed to produce a visible EL emission in this structure.

Figure 2 illustrates a typical current–voltage (*I–V*) characteristic of the OLEDs used in this study. The *I–V* curve indicates a diode-like behavior, with an ON/OFF current ratio greater than $10^3$ at $\pm 25$ V. No light emission has been observed when the reversed bias was applied to the diode structure, i.e., Al was positively biased with respect to ITO. Under the forward bias conditions, i.e., ITO is positively biased with respect to Al, the light emission occurred when the applied voltage was greater than $\sim 7$ V. The normalized electroluminescence spectrum, measured by the CCD system, is shown in Fig. 2 inset. The EL spectrum shows a peak located at around 545 nm with a full width at half maximum of about 80 nm.

The electroluminescence of the OLED induced by different operating current densities has also been studied. Figure 3 shows the OLED spectral distribution of luminance at different current densities. The shapes of all EL spectra are almost identical to each other with a minor exception at lower current densities, where the vibration modes contribute to the EL spectrum at higher wavelength. This results in a peak shoulder at low current densities. The brightness versus current density plot, shown in Fig. 3 inset, indicates a nearly linear relationship between luminance (obtained through integration of the area under peak at different current density)

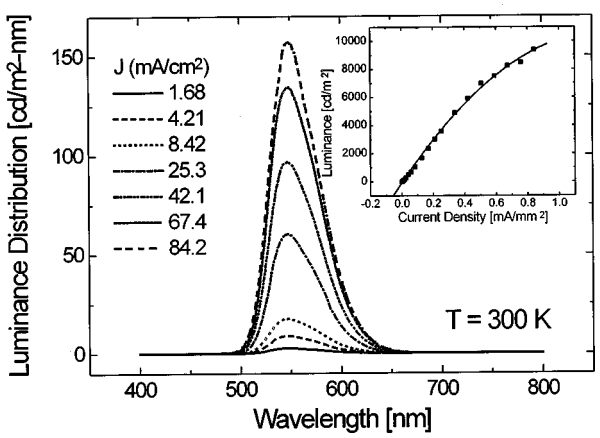


FIG. 3. Spectral distribution of the OLED luminance under different operating current densities. The inset shows the OLED brightness vs current density.

and current density at low current densities and a gradual luminance saturation at current densities higher than 0.7 $mA/mm^2$ (luminance above 8000 $cd/m^2$).

Using data shown in Fig. 3 we calculated the emission efficiency of the OLED at different current density (Fig. 4).

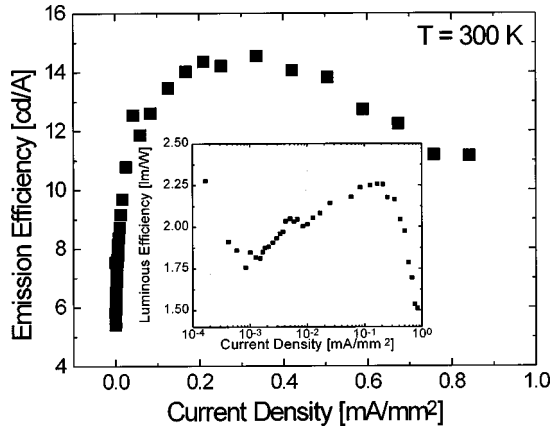


FIG. 4. Emission efficiency and luminous efficiency (inset) of the OLEDs at different current densities.

The emission efficiency increases rapidly at first then flats out and gradually drops with the increasing current density. The peak efficiency, 14.5 cd/A, appears at around 0.34 $mA/mm^2$ with $\sim$5000 $cd/m^2$ luminance. This peak efficiency gives the maximum external quantum efficiency of $\sim$3.86%. Figure 4 inset shows the luminous efficiency at different current density. The peak value (2.26 lm/W) emerges at about 0.17 $mA/mm^2$ with $\sim$2400 $cd/m^2$ luminance. This device exhibits excellent electrical stability even when operated at very high current densities ($>$250 $mA/cm^2$). The device stability will be reported in a different publication.

In conclusion, we have demonstrated a high performance bilayer (aminefluorene/benzothiadiazole-fluorene) organic polymer based light-emitting device using air-stable Al as the cathode material. Both the OLED luminance efficiency and the external quantum efficiency have been greatly improved in comparison with a single layer polymer based OLED. The use of the aluminum as the cathode material also provides an air-stable electrode that could be beneficial to final display integration.

The authors thank Professor Stephen Rand for important discussions. This research project is supported by the Center for Display Technology and Manufacturing at the University of Michigan. The organic polymers used in this study were provided by the Dow Chemical Company.

[1] J.H. Burroughes, D.D.C. Bradley, A.R. Brown, R.N. Marks, K. Mackay, R.H. Friend, P.L. Burn, and A.B. Holmes, Nature (London) **347**, 539 (1990).
[2] A. Dodabalapur, IEEE Trans. Electron Devices **44**, (1997).
[3] G. Yu, H. Nishino, A.J. Heeger, T.-A. Chen, and R.D. Rieke, Synth. Met. **72**, 249 (1995).
[4] F. Cacialli, R.H. Friend, N. Haylett, R. Daik, W.J. Feast, D.A. dos Santos, and J.L. Bredas, Appl. Phys. Lett. **69**, 3794 (1996).
[5] Y. Yang, Q. Pei, and A.J. Heeger, J. Appl. Phys. **79**, 934 (1996).
[6] L.S. Huang, C.W. Tang, and M.G. Mason, Appl. Phys. Lett. **70**, 152 (1997).
[7] N.C. Greenham, S.C. Moratti, D.D.C. Bradley, R.H. Friend, and A.B. Holmes, Nature (London) **365**, 628 (1993).
[8] R. Troutman, Synth. Met. **91**, 31 (1997).
[9] H.Y. Chu, D.H. Hwang, L.M. Do, and T. Zyung, Asia Display'98, 1998, p. 1091.
[10] N.C. Greenham, R.H. Friend, and D.D.C. Bradley, Adv. Mater. **6**, 491 (1994).